Solid-State ^{13}C-NMR Investigation of the Disorder in Crystalline Syndiotactic Polypropylene

Finizia Auriemma,† Ralf Born, and Hans Wolfgang Spiess*

Max-Planck-Institut für Polymerforschung, Postfach 3148, D-55021 Mainz, Germany

Claudio De Rosa and Paolo Corradini

Dipartimento di Chimica, Università di Napoli Federico II, via Mezzocannone 4, 80134 Napoli, Italy

Received December 27, 1994; Revised Manuscript Received July 24, 1995®

ABSTRACT: A quench-precipitated sample of highly syndiotactic polypropylene (s-PP) (with 86% fully syndiotactic pentads), which shows an X-ray spectrum near that calculated for an "ideal" orthorhombic C-centered structural model of packing as proposed by Corradini et al. (with chains in a helical $(TTGG)_n$ conformation), has been analyzed by high-resolution solid-state ^{13}C-NMR spectroscopy. The ^{13}C-NMR CP MAS spectra of this sample, in addition to the resonances already reported in the literature for s-PP (in the B-centered structure), exhibit additional peaks in the regions of the methyl (at 18.9 and 22.4 ppm) and methylene (at 44.9 ppm) groups. It is established that these additional resonances belong indeed to nuclei in well-defined conformational environments fixed in rigid structures placed at the interface of the crystallites and within the strained or disordered area of the crystallites themselves. In particular, the peak at 44.9 ppm in assigned to CH_2 carbon atoms in a TX.YG conformational environment, whereas the resonance at 18.9 ppm is assigned to CH_3 in *trans*-planar portions of the chain (*γ-gauche* effect). This indicates local disorder in the C-centered crystalline s-PP sample, due to the presence of conformationally disordered chains. Models of s-PP chains comprising defective but energetically feasible portions of chains in a *trans*-planar conformation (disturbing the $(TTGG)_n$ dominating conformation) are imagined as packed according to a C-pseudocentered structure. In order to keep the methyl groups in a crystalline register and the chains well interdigitated, the defects should be clustered on planes which cross 3D ordered portions in the crystals. The chemical shifts of the carbon atoms in the regions comprising the defect for model chains have been calculated on an *ab initio* level through the IGLO method, and the results are compared with the experiments. The calculations provide a good explanation of the peculiarities of the experimental ^{13}C-NMR spectra of the s-PP sample under study. Thus, detailed information on chain defects can be obtained by combining X-ray scattering, solid-state NMR, and computer simulations.

Introduction

Disorder phenomena are frequently observed in crystalline polymers. They correspond to the maintenance of the tridimensional positional order in the long range of only some of (and not of all) the coordinates characterizing the structure.[1] Diffraction techniques are sensitive to the presence of disorder in the crystalline structures. For instance, as a result of the presence of the disorder, some (h,k,l) reflections may appear more or less broad, streaked, or asymmetric.

We shall designate as "limit ordered structure" an idealized description in a given space group, resulting in a fixed position of all the (carbon) atoms in the crystal; we shall include in the expression "limit disordered structure" an idealized description in a space group, with statistical occupancy of some or all of the equivalent positions. These definitions rely on concepts extensively discussed in ref 1 (see mainly pp 185–187) and were first explicitly used in ref 2 (p 5719f).

In crystals with disorder, the concepts of limit ordered structure and of limit disordered structure are both useful.[1] A limit ordered structure may correspond to the description of the actual relative position of atoms in the short range; its concept may be useful to interpret diffuse X-ray scattering phenomena. A limit disordered structure may be appropriate for the description of the relative position of atoms in the long range and the occurrence of sharp lines in diffraction experiments.

From the analysis of the diffuse scattering, it is possible to trace out models of the crystalline structures, comprising a statistical distributions of the disorder. Techniques for the calculation of the diffraction profiles, accounting for the presence of the statistical disorder in a crystalline structure, allow one to discriminate between different models, through comparison between the calculated and experimental diffraction profiles.[2,3] No information can be deduced *a priori* about the local disorder with the usual diffraction techniques, however.

In order to get more insight in the local disorder in the crystals, solid-state NMR spectroscopy is particularly suited as it is very sensitive to the structural details. Indeed, high-resolution solid-state NMR spectroscopy not only offers the possibility of one to enhance selectively the resonances in partially crystalline samples of the mobile (usually amorphous) and rigid (usually crystalline) components but also allows one to easily distinguish between atoms in different conformations and, although to a lesser extent, in different packing environments.[4,5]

Modern computing power and novel schemes for the calculation of NMR chemical shifts (like, for instance, "Individual Gauge for Localized Orbitals" (IGLO);[6–9] see also references therein) have proved to be very effective in predicting experimental chemical shifts, in a variety of chemical compounds[9] and, lastly, also in amorphous polymers.[10] The spread in ^{13}C-NMR chemical shifts in solid amorphous polyisobutylene is quantitatively reproduced in the calculations using the IGLO method on model oligomers in selected conformations, deduced

† Permanent address: Dipartimento di Chimica, Università di Napoli Federico II, via Mezzocannone 4, 80134 Napoli, Italy.

® Abstract published in *Advance ACS Abstracts,* September 1, 1995.

0024-9297/95/2228-6902$09.00/0

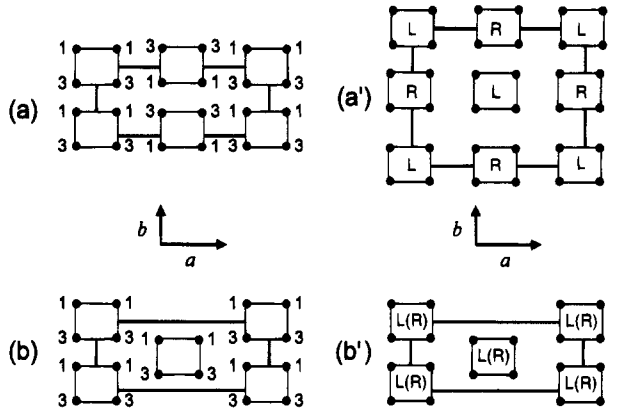

Figure 1. Packing models in the $a-b$ plane of macromolecular chains of s-PP, represented by rectangles in the case of a pseudocentered structure on the B face (a); in the case of a pseudocentered structure on the C face (b). The relative heights of the methyl groups (black balls, placed at the vertices of the rectangles) are in $c/4$ units. In a' and b' the chirality of adjacent chains are specified for the space groups *I*bca and $C222_1$, respectively. R = right-handed helix; L = left-handed helix.

from the conformational statistics as established in the literature for this polymer.[11]

This paper is concerned with the study of local defects in a crystalline form of syndiotactic polypropylene (s-PP) through solid-state ^{13}C-NMR spectroscopy. High-resolution solid-state ^{13}C-NMR spectra of this sample reveal the presence of a large amount of defects in the crystals, due to the presence of conformationally disordered chains. Possible kinds of defects in the chain backbone of s-PP are outlined. Models of s-PP oligomers, energetically feasible, comprising the defects are built up through the help of molecular mechanics. Hence, the chemical shifts of the carbon atoms in the regions comprising the defect of the model oligomers are calculated on an *ab initio* level through the IGLO method, and the results are compared with the experiments.

Description of the Polymorphism and of the Disorder of s-PP

Syndiotactic polypropylene (s-PP) may crystallize according to various polymorphic modifications,[12-16] and, depending on the degree of stereoregularity, the mechanical and thermal history of the samples shows different amounts of statistical disorder in the crystalline packing.[2,3,12,17-21] For the reader's convenience, some of the structural features of the different forms are reviewed here. In most of the commonly occurring polymorphic species, the chain conformations of s-PP has s(2/1)2 symmetry ($(TTG^+G^+)_2$, right-handed helix $(G^-G^-TT)_2$, left-handed helix); the helices are packed more or less disorderly according to one of the two orthorhombic models shown in parts a and b of Figure 1. The position of the chain axes and the relative height of the methyl groups of neighboring macromolecules characterize the two basic models of the mode of packing of the methyl groups: Figure 1a, B-centered axes in (0, 0, z) and ($^1/_2$, 0, z),[15] main X-ray peaks in the powder spectrum, at d = 7.25, 5.60, and 4.31 Å (2ϑ = 12.2°, 15.8°, 20.6°, Cu Kα); Figure 1b, C-centered axes in (0, 0, z) and ($^1/_2$, $^1/_2$, z), main X-ray peaks in the powder spectrum, at d = 7.25, 5.22, 4.31 Å (2ϑ = 12.2°, 17.0°, 20.6°, Cu Kα).[14]

The ideal limit ordered structures correspond to the orthorhombic space groups *Ibca*[18] (Figure 1a', helices of opposite chirality regularly alternate along a and b) and $C222_1$[14] (Figure 1b', all helices are isochiral), with identical a = 14.5 Å and c = 7.40 Å axes and with b = 11.2 Å (=5.6 × 2 Å) in Figure 1a' and b = 5.60 Å in Figure 1b'.

In all the structural limit models for $(TTGG)_2$ s-PP compatible with X-ray diffraction data, the maintenance of long-range order involves the positioning of the carbon atoms of the methyl groups, but not necessarily the positioning of the atoms of the chain backbone. Right- and left-handed helices have an identical outside envelope, as far as the methyl positions are concerned.[21]

Accordingly, the diffraction phenomena have been explained through models characterized by the following:[2,3,12]

(a) Departures from the regular alternation of the packing of TTGG helices of opposite chirality along a and b in the case of s-PP samples showing the characteristics of B-pseudocentered structures.

(b) Departure from the fully isochiral packing of TTGG helices in the case of s-PP samples showing the structural features of C-pseudocentered structures.

(c) A statistical mixture within the same crystal, of the B- and C-pseudocentered modes of packing of parts a and b of Figure 1. This kind of disorder has been observed in single crystals of s-PP obtained at low temperature,[18,19] as well as in fiber and powder specimens of s-PP.

Models of the disorder in which some kind of local order in maintained (e.g., the chirality of the first neighboring macromolecules) have been shown to be more appropriate, in order to explain the diffraction phenomena of s-PP samples studied.[2]

The possibility that the disorder in some crystals of s-PP originates from conformational defects is here examined. If such defects are present, they can, at least in principle, be detected through high-resolution solid-state NMR spectroscopy.

s-PP also presents a polymorph with chains in the *trans*-planar conformation,[13] obtained by cold drawing the polymer quenched in ice water from the melt. The structure, described by Chatani[22] for purposely prepared fibers, corresponds to chains organized in an orthorhombic lattice, centered on the C-face, with a = 5.22 Å, b = 11.17 Å, and c = 5.06 Å (chain axis). The main peaks in a hypothetical X-ray diffraction powder pattern would occur at d = 5.58, 4.73, and 3.75 Å (2ϑ = 15.9°, 18.8°, 23.7°, Cu Kα).

Another crystalline form, still described by Chatani,[16] has been obtained upon exposure of fiber specimens of s-PP initially in the *trans*-planar form, to suitable solvents at room temperature. It is characterized by helices in a $(T_6G_2T_2G_2)_n$ conformation. A triclinic cell has been proposed for this polymorph with a = 5.72 Å, b = 7.64 Å, c = 11.6 Å (chain axis), α = 73.1°, β = 88.8°, and γ = 112.0°. The hypothetical X-ray diffraction powder spectrum of this form would present main peaks at d = 6.84, 5.26, and 4.46 Å (2ϑ = 12.9°, 16.8°, 19.9°, Cu Kα). As outlined by Chatani in ref 16, this form is transformed readily to the form with the helices in the $(TTGG)_n$ conformation by annealing above 50°.

Experimental Section

The s-PP was supplied by "Himont Italia". The polymer was synthesized with syndiospecific homogeneous catalysts based on a column 4 (group 4A) metallocene/methylaluminoxane system according to the procedure explained in ref 23. The studied sample (M_w = 120 × 10^3) was obtained by performing the polymerization at 44 °C (it corresponds to sample 5 of ref

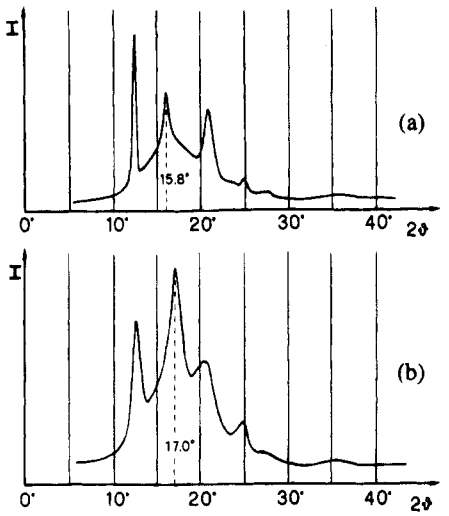

Figure 2. X-ray powder diffraction profiles of s-PP samples: (a) compression-molded sample (slowly crystallized from the melt, fully helical sample; (b) quench-precipitated sample (i.e., crystallized by precipitation with methanol from a solution in *n*-pentane and vacuum treated for 12 h at 60 °C).

22). The material is highly syndiotactic; in fact, the ^{13}C-NMR spectrum, recorded on a Bruker AC 300 spectrometer at 393 K in deuterated tetrachloroethane, gives the following distribution of pentads: 86% (*rrrr*); 5% (*rmrr*); 2% (*rrmm*); 6% (*mrrr*); 1% (*rmmr*).

The sample referred to in the following as "quench-precipitated" was obtained from the polymerization medium (*n*-pentane solution) by precipitation with CH_3OH/HCl and hence dried under vacuum at 60 °C for 12 h. The sample referred to in the following as "compression-molded" was slowly crystallized from the melt by heating the sample up to ≈200 °C under a press and successively cooling to room temperature at a cooling rate of 1.5 °C/min. This sample corresponds to a crystalline form with chains in fully helical $(TTGG)_n$ conformations.

The glass transition temperature T_g of the polymer as determined by differential thermal calorimetry on a Mettler DSC apparatus (heating rate 10 K/min) is 272 K.

Wide-angle X-ray diffraction spectra were obtained with nickel-filtered Cu Kα radiation, with an automatic Philips diffractometer.

The ^{13}C-NMR 1D MAS spectra were recorded at a spinning speed of f_{ROT} = 5 kHz on a Bruker ASX-500 spectrometer (^{13}C frequency: 125.76 MHz). The ^{13}C NMR 2D MAS spectra were acquired at a spinning speed of f_{ROT} = 3 kHz on a Bruker MSL 300 spectrometer (^{13}C frequency: 75.47 MHz). Adamantane was used as an external reference at 38.5 ppm relative to tetramethylsilane (TMS). All chemical shifts are given relative to TMS with an uncertainty of ≈0.5 ppm. For CP MAS spectra, in agreement with literature,[24] the best contact time was found to be approximately 2 ms. The pulse sequence for CP MAS 2D exchange NMR is described in detail elsewhere.[25]

Experimental Results and Discussion

X-ray Diffraction Data. Figure 2 compares the X-ray diffraction powder profiles of the compression-molded (fully helical) sample (Figure 2a) and of the quench-precipitated s-PP sample (Figure 2b). These patterns show a degree of crystallinity on the order of ≈40% and indicate the presence of a high degree of disorder in the crystalline regions (see refs 2, 3, and 12).

It is possible to associate the sample obtained after compression molding, with the B-centered structure (Figure 1a), whereas the quench-precipitated sample appears to be nearer to the C-centered structure (Figure 1b). This is indicated by the presence of (i) a strong peak at $2\vartheta = 15.8°$ with Miller indices 010 (unit cell with

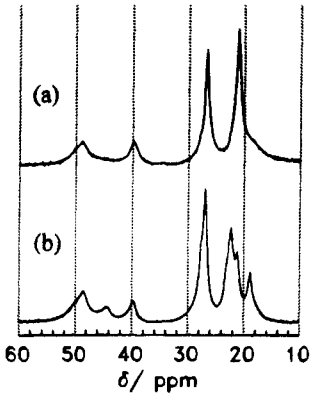

Figure 3. Solid-state ^{13}C-NMR CP MAS spectra (contact time 2 ms) at room temperature of (a) the compression-molded, fully helical s-PP sample and (b) of the quench-precipitated s-PP sample.

axes a = 14.5 Å, b = 5.60 Å, and c = 7.40 Å), in the diffractogram of Figure 2a and (ii) a strong and broad peak with the maximum at $2\vartheta = 17.0°$, indexed as 110 (the same unit cell constants as before), in the diffractogram on Figure 2b.[12]

Solid-State ^{13}C-NMR Data. Figure 3 shows the solid-state ^{13}C-NMR CP MAS spectra obtained for the two samples of s-PP at room temperature and with a contact time of 2 ms: compression-molded (fully helical) sample (Figure 3a); quench-precipitated sample (Figure 3b). The four peaks located at 21.3, 26.7, 40.2, and 49.1 ppm in the compression-molded (fully helical) sample (Figure 3a) correspond to the four peaks of crystalline s-PP already reported in the literature.[24,26] These four resonances are attributed to the methyl, to the methine, and, the latter two, to the methylene carbon atoms in the two conformational environments GT.TG and TG.GT, respectively (where the dot identifies the position of the CH_2, in a given sequence of dihedral angles).[24]

The spectrum of the quench-precipitated sample (Figure 3b), however, in addition to the main four peaks listed above shows two additional peaks in the region of the methyl groups at ≈18.9 and ≈22.4 ppm and one additional peak at ≈44.9 ppm in the region of the methylene groups. Moreover, the methyl group resonance with the maximum at 22.4 ppm exhibits a shoulder at ≈23.4 ppm. Similarly, the methine group resonance shows a shoulder at ≈27.6 ppm. The intensities of the peak at 18.9 ppm and of the unresolved set of peaks comprised between 21.3 and 23.4 ppm are in the approximate ratio 1:5.

For the quench-precipitated sample, it is worth noting that the resonance in the methylene region at 44.9 ppm cannot be ascribed to exchange phenomena, i.e., *trans/gauche* transitions occurring with an exchange rate much higher than the separation (in frequency units) between the resonances at 40.2 and 49.1 ppm.[25,27] Indeed, ^{13}C NMR CP MAS spectra recorded at temperatures much lower than the T_g of the quench-precipitated sample (203 K = T_g − 70 K) do not present substantial differences in the relative peak heights with respect to the spectrum of Figure 3b (recorded at room temperature) and with spectra recorded up to the temperature of 373 K (the spectra recorded at various temperatures, not shown here, will be reported in a forthcoming paper[28]). The absence of motional effects is shown even more clearly in Figure 4, where the ^{13}C-NMR 2D exchange CP MAS spectrum of the quench-precipitated sample recorded at room temperature, with a mixing time t_m = 500 ms, is reported. In such an

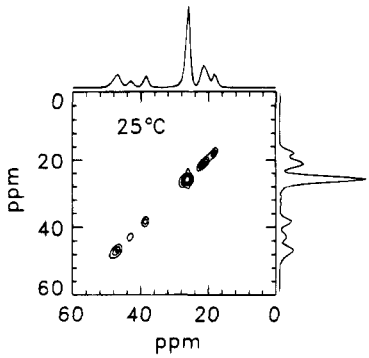

Figure 4. Solid-state ^{13}C-NMR CP MAS spectra of the quench-precipitated s-PP sample (contact time 2 ms) at room temperature: 1D spectrum (top and right side); 2D exchange spectrum with mixing time t_m = 500 ms (bottom). Contour lines with a constant value of the intensity, corresponding to 3%, 10%, 20%, 30%, and 50% of the absolute maximum in the spectrum.

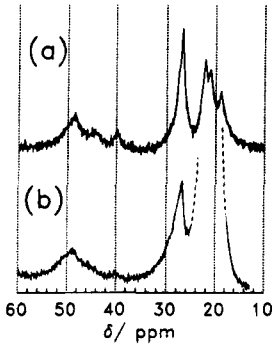

Figure 5. Solid-state ^{13}C-NMR MAS spectra at room temperature of the quench-precipitated s-PP sample with recycle times 100 s (a) and 1.5 s (b). In b, the dominant methyl region has been cut.

experiment[25] a mixing time t_m is inserted between the evolution time t_1, where a given ^{13}C spin evolves with frequency of ω_1, and a detection time t_2, where the same spin evolves with a frequency ω_2. If the frequency of a given nucleus is the same before and after the mixing time ($\omega_1 = \omega_2$), the signal is confined to the diagonal, with a line shape corresponding to that of the 1D spectrum. If a conformational transition occurs close to the given nucleus, different frequencies before and after t_m lead to off-diagonal cross peaks. For the quench-precipitated sample, a diagonal spectrum is obtained (shown in Figure 4), indicating that exchange phenomena do not occur over a mixing time as long as 500 ms. The same holds up to the temperature of 373 K (the spectra, not reported here, will be reported in the forthcoming paper[28]). The mixing time chosen in this experiment is consistent with the mixing times used in a variety of exchange experiments, to detect exchange phenomena in helical structures of synthetic polymers (1 ms to 1 s).[25]

In order to unravel the nature of those additional resonances, in Figure 5 we show the ^{13}C-NMR MAS single-pulse spectra of the quench-precipitated sample obtained with a long recycle time (100 s; Figure 5a) and a short recycle time (1.5 s, Figure 5b). Generally, in the spectra obtained with short recycle times, only the resonances of the nuclear species belonging to the most mobile phases appear, whereas in the spectra obtained with a long recycle time and proportions between the signals of different carbons, in the different phases, are close to the stoichiometric proportions.

We first note that the spectrum of Figure 5b is dominated by the methyl resonances, which have a short spin–lattice relaxation time T_1, due to the fast methyl rotation. No significant differences in the relative peak heights in this region are observed. However, in the methylene region the peaks at 44.9 and 40.2 ppm which are apparent in the spectra of Figures 3b and 5a are reduced in the spectrum of Figure 5b. Thus, they are possibly indicative of CH_2 groups in the crystalline phase of the quench-precipitated sample, while the peak at ≈49.1 ppm (present in all three spectra) is possibly due to CH_2 groups in both the crystalline and the amorphous regions.

It is worth noting that the methylene carbon atoms, giving rise to the three above-mentioned peaks, as well as the methine carbons, in the crystalline phase, exhibit T_1 on the order of tens of seconds, while the methyl carbon atoms, owing to their characteristic mobility around the C–C bond, show values of T_1 on the order of 1 s, independent of the rigidity of the phase. This is in agreement with literature data, for s-PP,[24] but also for isotactic polypropylene in the α and β crystalline modifications.[29]

We recall that the presence of the additional resonance at ≈45 ppm in the ^{13}C-NMR CP MAS spectrum of a crystalline s-PP sample obtained with the same catalyst systems as those used in the present paper was already reported in ref 24. The authors attribute this resonance to CH_2 nuclei in a TT.TG conformation, fixed in rigid structures placed at "the interface of the crystallites and within strained or disordered areas of the crystallites themselves".

The marked difference in the spectra of Figure 3 of the two samples of s-PP indicates, in fact, the possible presence of conformational defects of the kind proposed in ref 24. Indeed, the extra peak in the methylene region for the quench-precipitated sample can be easily attributed to a well-defined conformational environment for the methylene group. According to the rule that the effect of the conformation on the chemical shift is mainly due to the rotation about the next-neighboring bond, (*γ-gauche* effect)[30–32] the chemical shift of a given carbon atom may be evaluated empirically, by an additive contribution of ≈−4 ppm for each next-neighboring bond in a *gauche* state, in comparison with a *trans* state. Since the extra peak of resonance at ≈44.9 ppm for the methylene group is ≈−4 ppm upfield with respect to the peak attributed to CH_2 in a TG.GT conformational environment, it should be associated to a CH_2 in a GX.YT or TX.YG conformational sequence. From the spectrum of Figure 3b, we estimate the fraction of CH_2 giving rise to the resonance at ca. 44.9 ppm to be on the order of 10% of the total.

As far as the methyl region is concerned, the resonance of the CH_3 groups in crystalline s-PP samples with the chains in the *trans*-planar conformation is at ≈19.5 ppm.[33] Since in the quench-precipitated sample a resonance at 18.9 ppm and an unresolved set of resonances between 21.3 and 23.4 ppm are present, the conformational disorder in our sample is probably connected with the presence of portions of the chain in the *trans*-planar conformation in chains in a prevailing $(TTGG)_n$ conformation. As is well-known from the literature,[29] the packing can influence the chemical shift of the methyl groups. The presence of the three maxima at 21.3, 22.4, and 23.4 ppm instead of a single peak at 21.3 ppm[24,26] is probably due, however, also to displacements of bond lengths and valence and torsion angles

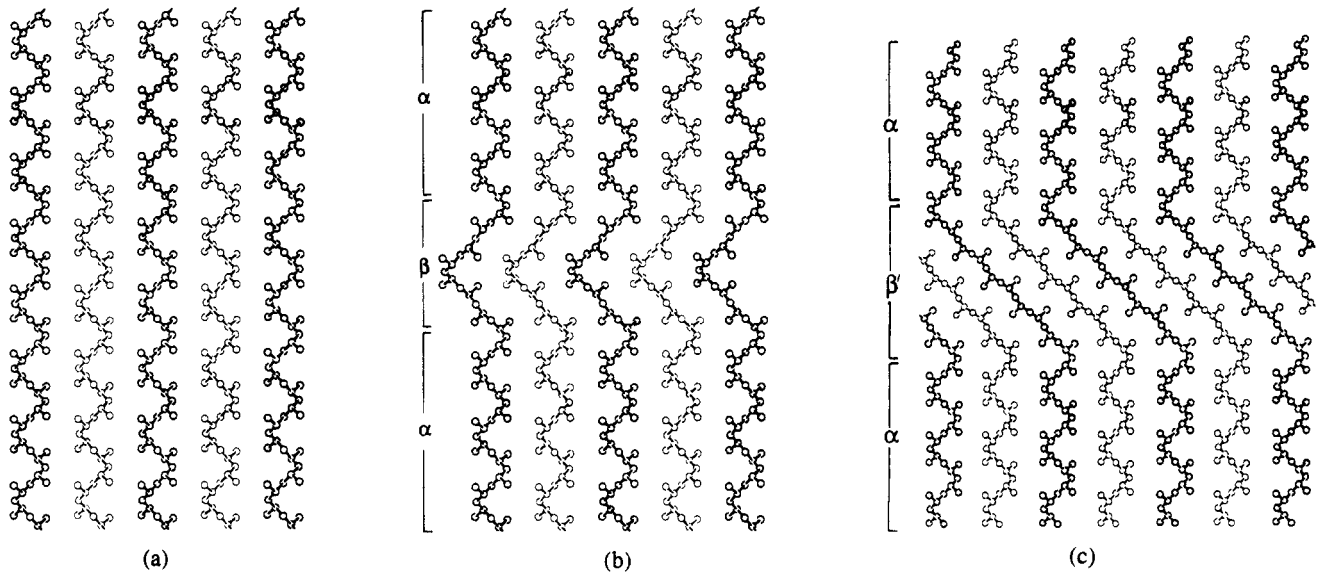

Figure 6. $a-c$ projection of C-centered structures: ordered case (space group $C222_1$) (a); two examples of disordered cases (b and c). Chains drawn with thin and bold lines are at 0 and $1/2$ along b (perpendicular to the plane of the drawing). In b and c, the portions of the chains in the regions indicated with α are in a s(2/1)2 conformation and have methyl groups in the crystallographic register, like in Figure 6a. The "defective" portions β of the chains in b correspond to a conformation $G_2T_6G_2T_6$; the defective portions β' in c to a conformation G_2T_{18}. The portions of the chains connected across the defective regions are isomorphic. The chain defects in b and c are thought as clustered along planes which cross a C-centered (otherwise regular) structure.

from the ideal values in a regular portion of the chain in helical s(2/1)2 symmetry, close to the conformational defects. The presence of *trans*-planar portions of chains also implies the presence of some CH_2's in a TT.TT conformational environment. According to the literature, the latter present a resonance at ≈50.2 ppm.[33] Since the peak at 49.2 ppm in the spectrum of Figure 3b is very broad, it can be interpreted as due to the overlap of the resonances relative to CH_2 groups in TT.TT and TG.GT conformational environments.

Possible Models of Disorder in the Crystals of the Quench-Precipitated Sample. The X-ray diffraction pattern (Figure 2b) of the quench-precipitated sample with a broad peak at $d = 5.22$ Å ($2\vartheta = 17.0°$) is indicative of disorder in a prevailingly C-pseudocentered structure (Figure 1b).[2,12] On the basis of the solid-state ^{13}C-NMR spectrum of Figure 3b, we suggest that such disorder originates from conformational defects, due to the presence of *trans*-planar portions, in chains with a prevailing $(TTGG)_n$ conformation.

It is worth noting that the ^{13}C-NMR CP MAS spectrum of s-PP in the crystalline form described by Chatani in ref 16, with chains in a $(T_6G_2T_2G_2)_n$ regular conformation, has been recently published by Sozzani et al.[34] This spectrum, although resulting from a mixture of crystals in different structures, presents the typical resonances of a s-PP chain in a $(T_6G_2T_2G_2)_n$ conformation. More precisely, in this spectrum peaks at 40.2, 44.6, 49.0, and 50.2 ppm are present, due to CH_2 groups in conformational environemts GT.TG, TT.TG, TG.GT, and TT.TT, respectively. Also, peaks at 19.8 and 23.2 ppm are present, due to CH_3 groups belonging to the portions of the chain in *trans*-planar and $(TTGG)_n$ conformations, respectively.

In the ^{13}C-NMR CP MAS spectrum of the quench-precipitated sample in Figure 3b of this paper, similar resonances are present. Although the presence of crystals in the B-pseudocentered orthorhombic structure as well as in the form described by Chatani in ref 16 cannot be completely excluded in our sample, we believe that the latter should not be present in a prevailing amount, for the following reasons:

(1) The X-ray diffraction profile of the quench-precipitated sample (Figure 2b) is typical of an orthorhombic C-pseudocentered structure, with chains in a prevailing helical conformation $(TTGG)_n$. In particular, the first diffraction peak in our case occurs at $2\vartheta = 12.4°$. Although in a structure like that one described by Chatani[16] with all the chains in the $(T_6G_2T_2G_2)_n$ conformation a strong diffraction peak at $2\vartheta = 17.0°$ would be present (in analogy with the quench-precipitated sample), the first diffraction peak would occur at $2\vartheta = 12.9°$.

(2) The diffraction profiles, as well as the ^{13}C-NMR CP MAS spectra of our sample obtained at different temperatures, do not present substantial differences up to 100 °C. As described in detail in a forthcoming paper,[28] the resonances at 44.9 ppm (methylene region) and at 18.9, 22.4, and 23.4 ppm (methyl region) disappear completely only upon melting (140 °C). For the structure with chains in the $(T_6G_2T_2G_2)_n$ conformation, instead, it is known from the literature[16,34] that it transforms in the more common crystalline forms with $(TTGG)_n$ chains, on heating the sample at $T \geq 50$ °C.

From the analysis of the experimental data of the preceding sections, it results that the conformational disorder in the quench-precipitated sample of this paper is in somehow connected with the presence of portions in the *trans*-planar conformation, in chains with a prevailing $(TTGG)_n$ conformation. In parts b and c of Figure 6 the $a-c$ projection of possible models of locally disordered structures, able to explain the experimental data, are shown, and in Figure 6a, for comparison, the $a-c$ projection of an ideal ordered structure is drawn. In all three structural models, the chains are packed in an orthorhombic lattice centered on the C face. In the disordered models of parts b and c of Figure 6 the chains are characterized by portions of chains in the helical conformation in an ideal symmetry s(2/1)2 (α portions). All of them are isochiral and are connected by portions

of chain in a $G_2T_6G_2T_6$ conformation (Figure 6b, β portions) or G_2T_{18} (Figure 6c, β' portions) in such a way that a substantial parallelism among the chain axes and the mean periodicity along the chain axis (7.40 Å) is maintained. In the regular portions of the chain the position of the methyl groups is the same as in an ideal crystal with $C222_1$ symmetry (compare parts b and c of Figure 6 with Figure 6a). Near to the "defective" planes (regions α and β) portions of chains in a $T_2G_2T_6$ conformation may be distinguished. They are similar to the conformational sequences in the structure described by Chatani in ref 16 and are packed in a similar manner. It is worth noting that the formation of plane defects β or β' corresponds to a very low cost of the chain conformational energy.[16,35] The chain defects modeled in parts b and c of Figure 6 do not seem to be easily mobile since they are clustered (and trapped) in planes (defect planes) as shown in the figure. The kinds of defects of parts b and c of Figure 6 mimic in many respects the "kink bands" described by Takahashi et al. in modifications II and I of poly(vinylidene fluoride).[36]

Each chain in a β defect comprises four methylene groups in a conformational environment GT.TT, giving the resonance at 44.9 ppm, two methylene groups in sequences TT.TT and two in sequences TG.GT corresponding to the resonance at 50.2 and 49.0 ppm, respectively. (Recall that the experimental peak around 49.2 ppm (Figure 3b) is very broad and can be interpreted as the overlap of these two conformational environments.) As far as the methyl groups are concerned, each β chain defect implies the presence of four CH_3 groups in a GG|TT chain environment (the vertical bar indicates a methyl group between two diads), which could explain the resonance at 22.4 ppm and four CH_3 groups in a TT|TT chain environment, which could explain the resonance at 18.9 ppm, i.e., ≈ -3 ppm upfield with respect to the resonance at 22.4 ppm (*γ-gauche* effect[30-32]).

In the same way, each β' chain defect implies two methylene groups in a conformational environment TT.TG, one methylene group in sequences TG.GT, and seven CH_2 groups in sequences TT.TT. As far as the methyl groups are concerned, eight CH_3 groups are found in sequences of the kind TT|TT, whereas two are in conformational environments TT|GG. The presence of defects β or β', one every 30–40 monomeric units, could quantitatively explain the features of the solid-state ^{13}C-NMR spectrum of Figure 3b.

The next section of this paper is aimed at the modeling of chains comprising these defects. Hence, the chemical shifts of the carbon atoms of the resulting model chains calculated through the IGLO method will be compared with the experimental data.

As suggested in ref 2, conformational disorder may also arise from the presence along the same chain of inversions in the sense of spiralization of the helices (trapped or mobile). Therefore, we have extended the IGLO calculations also to the hypothetical cases—which could occur for certain s-PP samples—of inversions arising from (and trapped to) a configurational defect of the kind *...rrrmrrrr...*, included in the crystalline lattice, or from a vacancy of a monomeric unit (see Figure 2 of ref 2) in an otherwise stereoregular chain (with the maintainance of the correlation in the position of the methyl groups in the enantiomorphic portions of the chain).

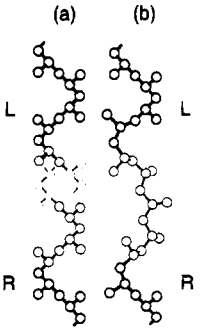

Figure 7. Schematic drawing of a left- (L) and right-handed (R) portion of a s-PP chain (a). The two portions are assumed to be coaxial; the methyl groups are in register with the crystallographic positions on both sides of the conformational inversion. The conformational inversion occurs through the "vacancy" of a monomeric unit (b).

Chain Modeling and Calculation of the Chemical Shifts

Since in nonconjugated systems the chemical shifts are most sensitive to the local geometry, short pieces of isolated model chains corresponding to the hypothesized conformational defects were chosen for the calculation of the chemical shift. It has been shown in ref 10 that even the effect of δ-neighboring atoms along a polymer chain on the calculated chemical shift of a given atom is already small, compared with the influence of γ-neighboring atoms.

For the model chains representing the kind of defect of parts b and c of Figure 6 the bond lengths and the valence and torsion angles were fixed to the values of the s-PP chains in the conformation $(T_6G_2T_2G_2)_n$ of ref 16, simply by arranging the various portions of those chains, in a different array. Of course, the geometry in the region of the defect was adjusted in order to maintain the same chain axis among the α portions of the chain, separated by the β or β' portions.

For the model chains comprising a vacancy of a monomeric unit, two segments of the chain in a regular s(2/1)2 helical conformation, ...$G^+G^+TTG^+G^+$ (right) and $G^-G^-TTG^-G^-$... (left), are juxtaposed coaxially and with the methyl groups in a crystallographic register, as shown in Figure 7a. They are joined through a sequence of the kind TG^-TTTTG^+T as in Figure 7b. For all the selected model chains, a minimization of the conformational energy was performed to adjust the local geometry (including the hydrogen atoms) on the isolated chains by using the Consistent Valence Force Field (CVFF) provided with the INSIGHT/DISCOVER (Version 2.9) package of BIOSYM, Inc.

For the selected geometries, an IGLO calculation was performed with the following Huzinaga basis of double-ζ quality (DZ, in the notation of ref 7): carbons were equipped with a (7s,3p) set in the contraction (4,1,1,1;2,1) and hydrogen with (3s) contracted to (2,1). As discussed in ref 10, although the DZ basis does not always yield satisfactory results, it works well in saturated hydrocarbons like s-PP, especially if the main interest is in the relative chemical shifts of a given group in different conformers.

The calculations yield σ values on an absolute scale σ, which is related to the experimental value δ by the relation $\delta = \sigma_0 - \sigma$, where σ_0 is the (absolute) shielding of a reference system (e.g., TMS). As discussed in ref 10, we adjusted the displayed range of δ for CH_3, CH_2, and CH independently, to allow an easy comparison of experimental and theoretical results.

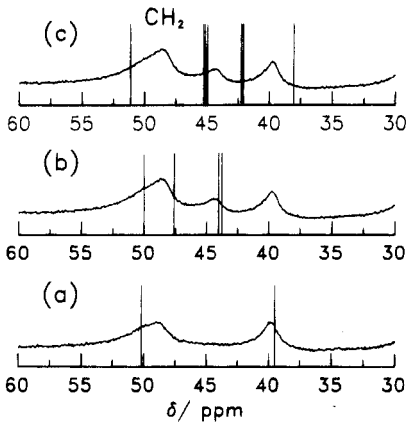

Figure 8. (a) Experimental ^{13}C-NMR CP MAS profile of the compression-molded (fully helical) sample (contact time 2 ms) in the methylene region. The bars are relative to the δ values calculated in the case of model chains of s-PP in a regular helical conformation, with internal coordinates taken from the literature.[35] b and c Experimental ^{13}C-NMR CP MAS profile of the quench-precipitated sample (contact time 2 ms) in the methylene region; in b the bars are relative to the values of δ calculated for the model chains of s-PP of Figure 6b in the β region; in c the bars are relative to the model chains of s-PP comprising a vacancy of a monomeric unit of Figure 7b in the β' region.

The calculations were performed on a DIGITAL DEC AXP 3000 Model 600 equipped with 64-MB core memory. We used the semidirect version of the program; routinely, for an oligomer comprising 12 monomeric units, ≈90 million integrals (≈40 million for hexamers) were stored on hard disk. A calculation for a single dodecamer conformation took roughly 18 h of CPU time (only 2 h for hexamers) in the DZ basis used for the calculation.

The calculated chemical shifts are reported for carbon atoms placed in the central region of the model oligomer, i.e., at least 5 atoms apart from the terminating carbon atoms of the model chain. We have checked that the calculated chemical shifts of the carbon atoms in the models correspond to those calculated for longer chains, provided that only the chemical shifts of the carbon atoms in the central region of the models are taken, as explained above.

Results of the Calculations of the Chemical Shifts and Discussion

For the calculated values of δ, a spread over a range of 1−2 ppm was found for a variation in both bond lengths (or valence angles) and oscillations of 10−20° of the dihedral angles. Since we present only the calculations for a few selected geometries, the values of δ calculated here should be considered a good approximation of the experimental values within a range of 1−2 ppm.

The results of the chemical shift calculations for the methylene carbon atoms are described in parts a−c of Figure 8 and compared with the experimental ^{13}C-NMR CP MAS spectra of the compression-molded sample (fully helical) (a) and of the quench-precipitated sample (b and c).

In Figure 8a the vertical bars represent the calculated values of δ of the methylene carbon atoms, in the case of an ordered model of s-PP in a s(2/1)2 symmetry, with the bond lengths and the valence and torsion angles fixed according to the value of the literature of ref 35, as an example. They are drawn by superimposing the solid-state ^{13}C-NMR profile of the compression-molded sample, with chains in a fully helical conformation (from Figure 3a), and are in good agreement with the experiment.

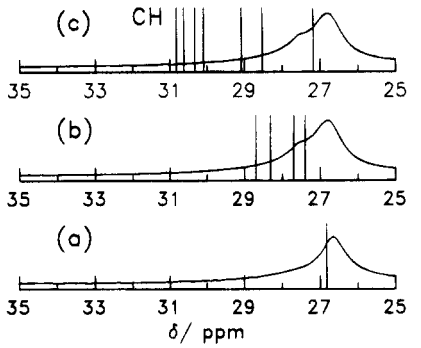

Figure 9. Analogous to Figure 8 for the methine carbon atoms.

The values of δ calculated for the disordered models of s-PP chains of Figures 6b and 7b are shown in parts b and c of Figure 8 for the methylene carbon atoms, respectively. Only the values of δ calculated for the carbon atoms in the diads constituting the defect are displayed.

The methylene region is the most important one in the spectrum of the quench-precipitated s-PP sample, since, owing to the *γ-gauche* effect, the chemical shifts are spread over an interval as large as 10 ppm, and the separation between the different peaks is 4 ppm, well beyond the error (1−2 ppm) of our approach. The error is largely due to the arbitrariness in choosing minor geometrical parameters of the chain which is to represent the defect. Special emphasis should be placed on whether or not the additional peak at δ = 44.9 ppm is reproduced.

As predicted before on empirical grounds, for the model of Figure 6b (β defect), four CH_2 groups exhibit chemical shifts around 45 ppm (some vertical bars overlap), being in a conformational environment TT.TG; two CH_2 are found in a conformational environment TT.TT and two CH_2 in TG.GT, with chemical shifts around 50 and 49 ppm, respectively.

As far as the model in Figure 7b is concerned, the conformation is of the kind "left-handed helix−$G^-G^-TG^+$-$TTTTG^-TG^+G^+$−right-handed helix". Hence, four CH_2 groups are found in a *TX.YG* conformational environment (see Figure 8c). More precisely, we find two methylene groups in two symmetrical conformational environments $G^-T.G^+T$ and $TG^-.TG^+$. They both correspond to calculated values of δ equal to 42 ppm. Analogously a second pair of CH_2 is found in symmetrical conformational environments $G^+T.TT$ and $TT.TG^-$, with calculated values of δ equal to 45 ppm. Thus, both disordered models reproduce the resonance at 45 ppm observed in the spectrum of the quench-precipitated sample.

The values of δ calculated for methine and methyl carbon atoms for the ordered model of s-PP in s(2/1)2 symmetry are reported in Figures 9a and 10a, respectively, in comparison with the ^{13}C-NMR CP MAS spectrum of the compression-molded (fully helical) sample. The values of δ calculated for the disordered models of Figures 6b and 7b are reported in parts b and c of Figure 9, respectively, for the methine carbon and in parts b and c of Figure 10 for the methyl carbon atoms. They are compared with the ^{13}C-NMR CP MAS spectrum of the quench-precipitated sample.

The calculated values of δ for the methine groups of the models in Figures 6b and 7b are spread in the

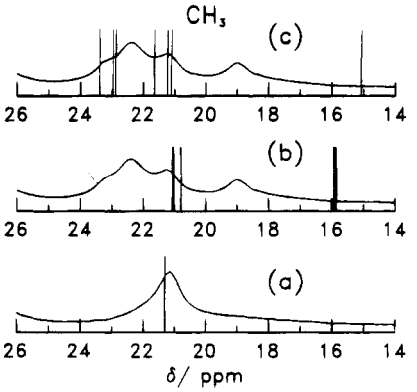

Figure 10. Analogous to Figure 8 for the methyl carbon atoms.

downfield region with respect to the resonance of CH carbon atoms belonging to a regular $(TTGG)_n$ chain (see Figure 9). This is in agreement with the experimental data for the quench-precipitated sample, which exhibit a methine resonance tailed in the downfield region as well.

As far as the methyl region is concerned (Figure 10), the agreement between the calculated and the experimental data is less satisfying than that for the methylene and methine regions. For instance, the calculated values of δ for the methyl groups in TT|TT portions of the chains are predicted around 16 ppm, 3 ppm apart from the resonance at 19 ppm, attributed in the literature to such kinds of CH_3 groups.[33] We observe that the IGLO calculations performed on a model chain with the internal parameters fixed according to the values given by Chatani for $(T_6G_2T_2G_2)_n$ regular chains[16] are in contrast with the experimental data[34] in a similar way. Indeed, the calculated values of δ for the methyl groups in TT|TT and TT|GG chain environments for a chain in a $(T_6G_2T_2G_2)_n$ regular chain are around 16 and 21 ppm, respectively, against the experimental values occurring around 20 and 23 ppm.[34] It is worth noting, as discussed above, that the chemical shifts of the methyl groups are significantly influenced by intermolecular, other than conformational, effects. The present approach, which completely disregards the influence of the packing on the calculated chemical shifts, cannot give more than a qualitative agreement with the experimental data, as far as the CH_3 groups are concerned.

Conclusions

In this paper a comparative study employing X-ray diffraction and high-resolution solid-state NMR augmented by molecular modeling allows one to elucidate the nature of local disorder in the crystals of the C-pseudocentered orthorhombic polymorph of s-PP (with chains in a helical s(2/1)2 conformation). The s-PP sample studied here is highly syndiotactic (the fully syndiotactic pentads are 86%).

On the one hand, the X-ray diffractogram of a powder sample of s-PP indicates the presence of a large amount of disorder in the crystals. On the other hand, the solid-state ^{13}C-NMR spectrum of the crystalline portion of this sample shows peculiarities, which, by use of semiempirical rules (γ-*gauche* effect) of the chemical shift, can be assigned to specific conformational defects in the crystals. More precisely, besides the resonance of methylene carbon atoms in the TG.GT and GT.TG conformational environment of s-PP chains in the s(2/1)2 conformation separated by about 9 ppm, an additional intermediate peak is found corresponding to a CH_2 in a TX.YG conformation. Analogously, besides the resonance at 21.3 ppm typical of the methyl groups in s(2/1)2 helices, additional resonances at 22.3 and 23.4 ppm (not resolved) and at 18.9 ppm are found. They are similar to the resonances of the methylene and methyl groups in some crystalline s-PP samples[33] with chains in a $(T_6G_2T_2G_2)_n$ conformation.[16]

For a quantitative analysis, model chains of s-PP comprising various kinds of defects are built up, through the help of the molecular mechanics, and the chemical shifts of the carbon atoms in the region surrounding the defect are calculated on the *ab initio* level through the IGLO method.

This shows that the possible origin of the local disorder in the quench-precipitated s-PP sample may originate from the presence of *trans*-planar portions of the chains connecting portions in a s(2/1)2 conformation.

The regular portions of the chains may be isomorphic, and in this case the chain defects are clustered in planes within the ordered regions in the crystals and are not mobile. The defect may be built up, as an example, by a portion of the chain in the conformation $(G_2T_{(4n+2)})_{2n'}$; the case $G_2T_6G_2T_6$ (Figure 6a) emulates the chain conformation in the crystalline form described by Chatani in ref 16. The defect may also be built up (again as an example) by a portion of the chain in the conformation $G_2T_{2(4n+1)}$ ($n = 0, 2, 4, \ldots$): the case G_2T_{18} is shown in Figure 6b. Defects of this kind allow one to preserve a substantial parallelism among the chain axes and a mean periodicity along the chain axes equal to 7.40 Å. In the resulting structures the chains would be packed according to an orthorhombic lattice centered on the C face: for the ordered regions, this corresponds to the ideal structure of Figure 6a (space group $C222_1$); in the regions comprising the defect, this leads to the structure described by Chatani[16,21] (Figure 6b,c).

Such disorder can account for the presence of the additional intermediate resonance at 44.9 ppm corresponding to a CH_2 in a TX.YG conformation. As far as the methyl groups are concerned, the calculated values of δ are only in fair agreement with the experiment, emphasizing that for the methyl carbon atoms, in addition to intramolecular effects, the packing can contribute to the complexity of the NMR pattern in the related region.[28]

Upon crystallization from the melt of the same sample, the B-pseudocentered orthorhombic structure occurs and the peculiarities in the solid-state ^{13}C-NMR spectrum disappear (only the resonances due to the methylene groups in a TG.GT and GT.TG conformational environment remain).[28]

Acknowledgment. We thank Dr. E. Albizzati and Dr. M. Galimberti of Himont-Italia for supplying the s-PP sample, U. Pawelzik for DSC analyses, P. Kindervater for ^{13}C-NMR spectra of the polymer in solution, and Dr. R. Lewis for his help in ^{13}C-NMR 2D CP MAS data collection. F.A. thanks the Consiglio Nazionale delle Ricerche of Italy, for having furnished a postdoctoral fellowship. We also thank the two reviewers for their specific suggestions on NMR assignments and defect structures, from which our manuscript has benefited.

References and Notes

(1) Corradini, P.; Guerra, G. *Adv. Polym. Sci.* **1992**, *100*, 183.

(2) Auriemma, F.; De Rosa, C.; Corradini, P. *Macromolecules* **1993**, *26*, 5719.
(3) Auriemma, F.; De Rosa, C.; Corradini, P. *Rend. Fis. Accad. Lincei* **1993**, *4*, supplement 9, 287.
(4) Voelkel, R. *Angew. Chem., Int. Ed. Engl.* **1988**, *27*, 1468.
(5) McBrierty, V. J.; Packer, K. J. *Nuclear Magnetic Resonance in Solid Polymers*; Cambridge University Press: Cambridge, U.K., 1993.
(6) Kutzelnigg, W. *Isr. J. Chem.* **1980**, *19*, 193. Schindler, M.; Kutzelnigg, W. *J. Chem. Phys.* **1982**, *76*, 1919.
(7) Kutzelnigg, W.; Fleischer, U.; Schindler, M. *NMR Basic Princ. Prog.* **1991**, *23*, 165.
(8) Kutzelnigg, W.; Wuellen, C. V.; Feischer, U.; Franke, R.; Mourik, T. v. In *Nuclear Magnetic Shielding and Molecular Structure*; NATO Advanced Study Institute Series C; Tossel, J., Ed.; Kluwer: Dordrecht, The Netherlands, 1993; Vol. 386, pp 141–161.
(9) Kutzelnigg, W. *J. Mol. Struct.* THEOCHEM **1989**, *202*, 11.
(10) Born, R.; Spiess, H. W.; Kutzelnigg, W.; Fleischer, U.; Schindler, M. *Macromolecules* **1994**, *27*, 1500.
(11) Vacatello, M.; Yoon, D. Y. *Macromolecules* **1992**, *25*, 2502.
(12) De Rosa, C.; Corradini, P. *Macromolecules* **1993**, *26*, 5711.
(13) Natta, G.; Peraldo, M.; Allegra, G. *Makromol. Chem.* **1964**, *75*, 215.
(14) Corradini, P.; Natta, G.; Ganis, P.; Temussi, P. A. *J. Polym. Sci., Part C* **1967**, *16*, 2477.
(15) Lotz, B.; Lovinger, A. J.; Cais, R. E. *Macromolecules* **1988**, *21*, 2375.
(16) Chatani, Y.; Maruyama, Y.; Asanuma, T.; Shiomura, T. *J. Polym. Sci., Polym. Phys.* **1991**, *29*, 1649.
(17) Lovinger, A. J.; Lotz, B.; Davis, D. D. *Polymer* **1990**, *31*, 2253.
(18) Lovinger, A. J.; Davis, D. D.; Lotz, B. *Macromolecules* **1991**, *24*, 552.
(19) Lovinger, A. J.; Lotz, B.; Davis, D. D.; Padden, F. J. *Macromolecules* **1993**, *26*, 3494.
(20) Stocker, W.; Schumacher, M.; Graff, S.; Lang, J.; Wittman, J. C.; Lovinger, A. J.; Lotz, B. *Macromolecules* **1994**, *27*, 6948.
(21) Corradini, P.; Napolitano, R.; Pirozzi, B. *Rend. Fis. Accad. Lincei* **1991**, supplement 9, *2*, 341.
(22) Chatani, Y.; Maruyama, H.; Noguchi, K.; Asanama, T.; Shiomura, T. *J. Polym. Sci., Part C: Polym. Lett.* **1990**, *393*, 28.
(23) Balbontin, G.; Dainelli, D.; Galimberti, M. *Makromol. Chem.* **1992**, *193*, 693.
(24) Sozzani, P.; Simonutti, R.; Galimberti, M. *Macromolecules* **1993**, *26*, 5781.
(25) Schmidt-Rohr, K.; Spiess, H. W. *Multidimensional Solid-State NMR and Polymers*; Academic: London, 1994.
(26) Bunn, A.; Cudby, E. A. *J. Chem. Soc., Chem. Commun.* **1981**, 15.
(27) Zemke, K.; Schmidt-Rohr, K.; Spiess, H. W. *Acta Polym.* **1994**, *45*, 148.
(28) Auriemma, F.; Lewis, R. H.; Spiess, H. W.; De Rosa, C. *Makromol. Chem.* **1995**, *196*, in press.
(29) Gomez, M. A.; Tanaka, H.; Tonelli, A. E. *Polymer* **1987**, *28*, 2227.
(30) Grant, D. M.; Cheney, B. V. *J. Am. Chem. Soc.* **1967**, *89*, 5315.
(31) Bovey, F. A. *Structure and Conformation of Macromolecules*; Academic Press: New York, 1982.
(32) Tonelli, A. E. *Spectroscopy and Polymer Microstructure: the Conformational Connection*; VCH Publishers: New York, 1989.
(33) Sozzani, P.; Galimberti, M.; Balbontin, G. *Makromol. Chem., Rapid Commun.* **1992**, *13*, 305.
(34) Sozzani, P.; Simonutti, R.; Comotti, A. *Magn. Reson. Chem.* **1994**, *32*, s45.
(35) Pirozzi, B.; Napolitano, R. *Eur. Polym. J.* **1992**, *28*, 703.
(36) Takahashi, Y.; Tadokoro, H. *Macromolecules* **1990**, *13*, 1316. Takahashi, Y.; Tadokoro, H.; Odajima, A. *Macromolecules* **1990**, *13*, 1318.

MA946386D